Astron. Astrophys. 321, 703–712 (1997)

ASTRONOMY
AND
ASTROPHYSICS

Anisotropic stellar systems with tangentially biased velocity dispersion

G. Bertin[1], **F. Leeuwin**[1], **F. Pegoraro**[1,2], **and F. Rubini**[3]

[1] Scuola Normale Superiore, Piazza dei Cavalieri 7, I-56126, Pisa, Italy (bertin@sns.it)
[2] Dipartimento di Fisica Teorica, Università di Torino, I-10125, Torino, Italy
[3] Dipartimento di Astronomia e Scienza dello Spazio, Università di Firenze, I-50125, Firenze, Italy

Received 23 November 1995 / Accepted 22 July 1996

Abstract. This paper provides a simple general procedure to construct self-consistent spherical equilibrium models of stellar systems populated by stars in quasi-circular orbits. The focus on Maxwellian-like distributions in the relevant velocity space and the use of the epicyclic expansion allow us to work with physically intuitive models. Explicit solutions for a sequence of distribution functions with density distribution close to that of isochrone models are produced with varying degrees of pressure anisotropy. These results are meant to be the starting point for extensive stability analyses, and they may also be of interest for the construction of quantities such as projected velocity dispersion and line-of-sight-velocity profiles for comparison with observations of elliptical galaxies.

Key words: galaxies: structure – galaxies: kinematics and dynamics – galaxies: elliptical and lenticular, cD

1. Introduction

Anisotropic equilibrium models of spherical, non-rotating stellar systems have been extensively investigated in recent years. Largely guided by physical arguments, N-body experiments, and observations, attention has generally been focused on systems with an excess of radial orbits (e.g., see Fridman & Polyachenko 1984; Bertin & Stiavelli 1993, and the many references quoted there).

A wide choice of self-consistent tangentially anisotropic models would be desirable for at least three reasons. It would be an important tool to further explore the stability of spherical collisionless stellar systems, for which the main interest so far has focused on the issue of the radial-orbit instability (Palmer 1994). Furthermore, it could provide a natural basis for fitting velocity dispersion profiles in elliptical galaxies when the observed radial decline is relatively slow; it is well known (Tonry 1983) that these cases can be interpreted as evidence for the existence of gradients in the mass-to-light ratios (see Bertin et al. 1994a), but that in principle they could be modelled as tangentially anisotropic equilibrium configurations with a constant mass-to-light ratio, as for example shown by Dejonghe (1989) through the use of polynomial distribution functions. Finally, in a related objective, a wide choice of tangentially anisotropic models would be interesting in order to construct synthetic line-of-sight velocity distribution functions for comparison with the observed line profiles (see Bender et al. 1994 and references therein).

In practice, there is only a rather limited choice of self-consistent tangentially anisotropic models. In particular, distribution functions dependent on one relatively straightforward combination of integrals of the motion (Osipkov 1979; Merritt 1985a, b) are well suited to the construction of radially anisotropic systems, but often fail when tried for the tangentially biased case (for example, they do not work for the isochrone models - see also Saha 1991). One useful assumption is to consider distribution functions that are separable in E (or J) and some other simple variable depending on E and J (Hénon 1973; Gerhard 1991; Cuddeford 1991; Louis 1993). For example, Gerhard (1991) has devised a general method for the construction of anisotropic stellar systems, based on a distribution function factorized as the product of a function of energy and a *circularity function*; the latter depends on a combination of energy and angular momentum and controls the distribution of orbits in the outer parts. For a given simple choice of the circularity function, such a factorization allows for an inversion determining the distribution function from a given density profile. Gerhard's models are isotropic in the central regions and reach constant anisotropy in their envelopes. In general, the models that are anisotropic at large radii have an isotropic core, while those that have tangential anisotropy in the center (Cuddeford 1991) are radially anisotropic in their envelopes.

In this paper we describe an alternative method specially aimed at the construction of self-consistent spherical stellar systems characterized by tangentially biased velocity dispersion with a given density distribution. This method appears to be

Send offprint requests to: G. Bertin

very simple from the physical point of view and fairly flexible. The construction starts with the case of systems populated mostly by quasi-circular orbits and identifies sequences of models with varying degrees of pressure anisotropy; these sequences can then be explored also in regimes where the pressure tensor becomes relatively close to being isotropic. In addition, there is significant freedom in the choice of the relevant anisotropy profile. The method is illustrated in detail for the case of an isochrone potential.

The main idea of our method is that of adapting the epicyclic procedure originally developed (Shu 1969) for rotating disks with a modified Schwarzschild (i.e., quasi-Maxwellian) distribution function to the different geometry of spherical, non-rotating stellar systems. Thus the method is physically intuitive. It turns out that the whole procedure can be carried through analytically, to the extent that the exact behavior of the models at small radii is judged to be unimportant. When one tries to complete the description by following the properties of the models all the way down to the center, one is forced to consider significant departures from the initially assumed density profile, and often some peculiar gradients are noted. Alternatively, a solution with the assumed density profile can be implemented, at the cost of completing the definition of the distribution function numerically. This is obtained by a suitable contour integration in the complex plane. Both methods are based on the smallness of the epicyclic parameter. The solutions that are found can be used as an input for stability analyses of the type described in a previous paper (Bertin et al. 1994b), i.e. linear modal analyses that require the knowledge of the dependence of the distribution function on the integrals of the motion.

In stellar dynamics many articles address the question of whether a given density profile can be generated exactly by a (positive definite) distribution function and some investigate all the possible forms of the distribution function that can serve such purpose (the "inversion" problem $\rho \rightarrow f$). It should be stressed that, in this respect, this paper addresses a completely different problem. In fact, since the stability of collisionless systems is known to depend primarily on the gradients of the distribution function in phase space and on the degree of pressure anisotropy (see Fridman & Polyachenko 1984), we give priority to a physically reasonable choice of the distribution function and show that wide classes of self-consistent solutions that yield the desired density profile, with a tangentially biased velocity pressure anisotropy, can be constructed with this procedure. The focus on Maxwellian-like distributions in the relevant velocity space serves the purpose of avoiding systems that might be affected *a priori* by "spurious" kinetic instabilities. For the same reason, we choose to avoid the construction of solutions with singular behavior at $r \rightarrow 0$. Such a behavior occurs naturally if we insist on loading circular orbits all the way down to the center. In fact, if we consider a distribution function made of purely circular orbits $f(r, v_r, v_\perp) = P(r)\delta(v_r)\delta(v_\perp - r\Omega(r))$ and integrate over velocity space to solve for $P(r)$, given a density $\rho(r)$, a difficulty arises at small radii for any regular density-potential pair, since $P(r) = \rho(r)/(2\pi r\Omega(r))$ so that $P(r)$, and thus the supporting distribution function, must be singular. Since singular models would be artificial and, again, might be subject to "spurious" instabilities, in this paper we avoid such a central singularity by allowing for an isotropic core.

2. Constructing a model with a tangentially biased pressure tensor

Following the procedure devised by Shu (1969) for the case of rotating disks, we consider systems made of stars for which the orbits are well described by the epicyclic approximation. In this case, for a given potential $\Phi(r)$, the radial coordinate r may be essentially identified with the angular momentum coordinate J, since stars are confined to a small annulus around the guiding center radius $r_0(J)$, with r_0 a monotonic increasing function of J. Thus we look for distribution functions that are significantly different from zero only for values of the energy E close to the minimum energy $E_{\min}(J) \equiv [r_0\Omega(r_0)]^2/2 + \Phi(r_0)$ characteristic of the circular orbit at r_0.

One possible choice for the distribution function is a quasi-Maxwellian function in the peculiar velocities with respect to the circular motion at speed $r_0\Omega(r_0)$:

$$f = P(r_0)\ \exp\left[-(E - E_{\min}(J))/c^2(r_0)\right], \tag{1}$$

with $f = 0$ for $E \geq 0$. Here J denotes the magnitude of the star specific angular momentum and the star specific energy is $E = v^2/2 + \Phi(r)$. This distribution function depends on two functions $P(r_0)$ and $c(r_0)$ of the angular momentum, which should be chosen in order for the system to be consistent with the potential $\Phi(r)$ and with the assumed epicyclic approximation. The latter requirement may be met if the quantity $c(r_0)$ is taken to be small: $c(r_0) = \epsilon\ \hat{c}(r_0)$, with ϵ a small dimensionless parameter such that

$$\frac{\epsilon\ \hat{c}(r_0)}{r_0\kappa(r_0)} \ll 1. \tag{2}$$

Here κ is the standard epicyclic frequency.

2.1. Models made of quasi-circular orbits

The Maxwellian distribution of peculiar velocities of the star orbits (with respect to the circular motions) associated with choice (1) for the distribution function can be recovered in the following way. First consider the distribution function expressed as a function $F(r, v_r, v_\perp)$. Then, introduce a transformation to the variables (r, v_r, w), where w is a peculiar tangential velocity defined by the relation $v_\perp^2 = r^2\Omega^2(r) + 2r\Omega(r)w + w^2$. Therefore, in the epicyclic approximation we have $r_0 - r \sim (2\Omega/\kappa^2)w$. Thus, by expanding $[E - E_{\min}(J)]$ around $r = r_0(J)$, the argument of the exponential in (1) becomes:

$$\frac{E - E_{\min}(J)}{c^2(r_0)} \sim \frac{v_r^2 + \kappa^2(r - r_0)^2}{2c^2(r_0)} \sim \frac{v_r^2 + (4\Omega^2/\kappa^2)w^2}{2c^2(r)}. \tag{3}$$

By approximating r_0 by r in the function $P(r_0)$ and integrating over velocity space, based on a saddle point method (under certain assumptions that turn out to fail at small radii – see Sect. 2.2 and Appendix A), we find an approximate relation between the function P and the mass density ρ: $P(r) \sim$

$\rho/(2\pi^2 r\kappa c^2)$, where all the functions appearing on the right hand side are meant to be functions of r. Thus we can start from this approximate relation and *define* the function $P(r_0)$ as:

$$P(r_0) = \frac{\rho}{2\pi^2 r_0 \kappa c^2}, \tag{4}$$

where all the functions appearing on the right hand side are now meant to be functions of $r_0(J)$.

The choice of the function $c(r_0)$ can be made so as to generate some desired anisotropy profile. Indeed, if we introduce the local anisotropy parameter $\alpha(r)$ as

$$\alpha(r) = 2 - \frac{\langle v_\phi^2\rangle + \langle v_\theta^2\rangle}{\langle v_r^2\rangle} = 2 - \frac{\langle v_\perp^2\rangle}{\langle v_r^2\rangle}, \tag{5}$$

we can write the hydrostatic equilibrium equation in the form:

$$\begin{aligned}\alpha(r) &= -\left(\frac{r^2\Omega^2}{\langle v_r^2\rangle} + \frac{d\ \ln\rho}{d\ \ln r} + \frac{d\ \ln\langle v_r^2\rangle}{d\ \ln r}\right)\\ &\sim -\left(\frac{r^2\Omega^2}{c^2(r)} + \frac{d\ \ln\rho}{d\ \ln r} + \frac{d\ \ln c^2(r)}{d\ \ln r}\right).\end{aligned} \tag{6}$$

In particular, this shows that, for a given density distribution, the local anisotropy parameter is $O\left(\epsilon^{-2}\right)$.

In conclusion, Eqs.(1) and (4), together with condition (2), are expected to form the basis for a distribution function that supports a cold distribution of quasi-circular orbits for a given choice of density ρ and potential Φ. When the coldness parameter ϵ is taken to be of order unity, the underlying physical picture that has guided our choice of f is bound to fail and problems are expected to be encountered when the Poisson equation is considered.

2.2. The problem at small radii

The physical picture outlined so far is based on an epicyclic approximation; the radial range of its validity depends on the choice of $\hat{c}(J)$. If we assume that condition (2) applies uniformly in J, then the function $c(r_0)$ must become vanishingly small at $r_0 \to 0$ for any assumed regular density distribution $\rho(r)$. This implies a singular behavior of the distribution function (1). [Note that this behavior does not depend on the specific choice of distribution function made, as is briefly shown in the Introduction.] In the following, we relax condition (2) at small radii, so that the distribution function f is regular, but then the choice of the function P given by Eq. (4) should be improved in order to take into account the orbits that are no longer quasi-circular at small values of the angular momentum. Note that if we require $c(r_0)$ to remain finite at $r_0 \to 0$, the epicyclic parameter appearing in (2) formally diverges, indicating that the central parts of the model will no longer be characterized by tangentially biased pressure and are presumably going to be isotropic.

To be more specific, if we refer to models characterized at large radii by Keplerian forces and constant anisotropy, a choice of $\hat{c}$ of the form

$$\hat{c} = \frac{J_1 J^{1/2}}{J_1^{3/2} + J^{3/2}}\sqrt{-2\Phi(0)} \tag{7}$$

gives rise to a singular distribution function, while a choice of the form

$$\hat{c} = \frac{J_1}{J_1 + J}\sqrt{-2\Phi(0)} \tag{8}$$

is going to lead to an isotropic core. In the above expressions J_1 is a reference angular momentum. Note from Eqs. (2) and (8) that the epicyclic approximation is expected to break down at radii $r \sim c/\kappa = O(\epsilon)$.

Based on choice (8), we may improve the definition of the normalization factor P as obtained from the saddle-point method by defining

$$P(r_0) = \frac{\rho}{2\pi^2 r_0\kappa c^2} \times g(r_0), \tag{9}$$

with $g(r_0) \sim (\pi/2)^{1/2} r_0\kappa/c$ at small values of the angular momentum, so that at the center it matches the normalization of an isotropic Maxwellian (see Eq. (29) and the discussion at the end of Appendix A). One relatively smooth choice for the function g is:

$$g(r_0) = \frac{r_0\kappa}{\left[(c\sqrt{2/\pi})^4 + (r_0\kappa)^4\right]^{1/4}}. \tag{10}$$

Note that since Eq. (4) (or Eq. (9)) is derived from a saddle-point method which breaks down at small radii (see Appendix A), the actual density given by $\int f\ d^3v$ may differ from the density ρ appearing in Eq. (4) (or Eq. (9)). In order to resolve this discrepancy, we may then consider two viable options. The first option (see following Sect. 2.3) is that of taking the integral of f to be the true density and, by an iterative procedure, to correct the value of the potential $\Phi(r)$ in order to satisfy self-consistency as required by the Poisson equation in terms of the true density. In this case, the final model turns out to be associated with a density–potential pair that may be appreciably different from that used to initialize the procedure. An alternative option gives priority to the initial choice of density distribution (and thus of the corresponding potential) and aims at improving definition (4) so that self-consistency is automatically guaranteed; in this case (see Sect. 2.4) the analytical definition (4) is replaced by one that involves a numerical evaluation of an integral.

2.3. Self-consistency

The definition of the distribution function (1) and (4) (or Eq. (9)) assumes the knowledge of the basic potential Φ (explicitly, in the energy dependence, and implicitly through the definition of the functions $r_0(J)$, $E_{\min}(J)$, $\kappa(r_0)$, and $\rho(r_0)$). If we follow the first option mentioned above, we may proceed iteratively as follows. We calculate the density $\rho^{(1)}$ from

$$\rho^{(1)} = \int f\ d^3v; \tag{11}$$

then we evaluate a corrected potential $\Phi^{(1)}$ from the Gauss theorem

$$\Phi^{(1)} = -G\int_r^\infty \frac{M^{(1)}(x)}{x^2}\ dx, \tag{12}$$

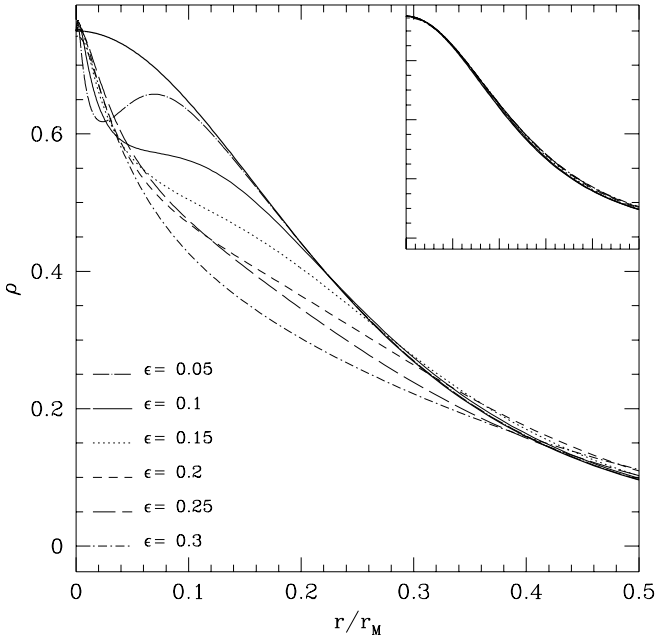

Fig. 1. Density profiles of the models with fixed functional form of distribution function (i.e., with $P(r_0)$ given by Eq. (9)), for various values of the ϵ parameter. The thick line is the isochrone density. The inset shows the density profiles for the corresponding models based on the contour integration method

with

$$M^{(1)}(r) = 4\pi \int_0^r \rho^{(1)}(x) x^2 \, dx. \tag{13}$$

A few steps should bring convergence to a self-consistent function. At each iteration step, self-consistency can be judged by testing the virial theorem.

In Sect. 3 we shall illustrate the properties of the models that are found following the asymptotic procedure described above by applying it to the case of isochrone potentials. As we shall show there in detail, in the case of small values of ϵ the models that are found present some undesired features in their density profile close to the center.

2.4. Inversion by contour integration

A different approach from the one outlined so far is that of looking for an approximate inversion procedure able to determine the normalization function P guaranteeing support to the assumed density distribution $\rho(r)$ *uniformly* at all radii. In other words, we would like to identify a function P of the angular momentum such that

$$\rho(r) \sim \frac{(2\pi)^{3/2}}{r^2} \int_0^\infty JdJ \; c(J) P(J) \times \exp\left(-\frac{\frac{J^2}{2r^2} + \Phi(r) - E_{\min}(J)}{c^2(J)} \right), \tag{14}$$

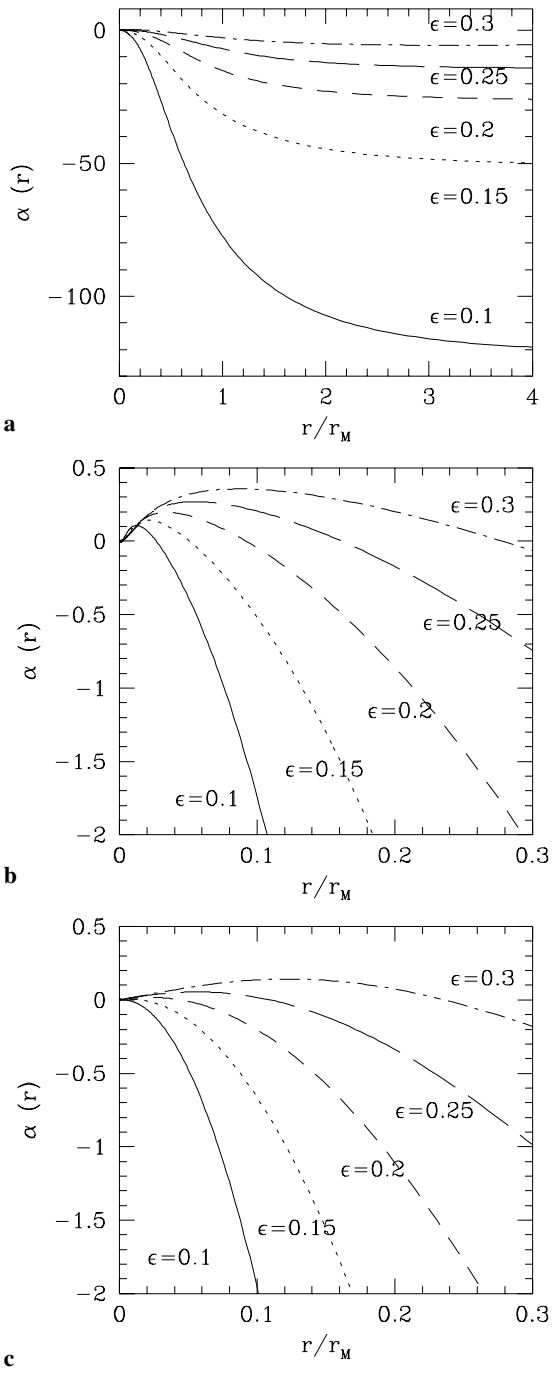

Fig. 2a–c. Profiles of the anisotropy parameter α for the models with fixed functional form of distribution function (**a** and **b**) and for the models based on the contour integration method **(c)**. Frames **b** and **c** focus on the central regions of the models

derived from the definition $\int f \, d^3v$ in Appendix A. Thus, the starting point of the inversion is the following equation:

$$u\rho(\sqrt{u}) = (2\pi)^{3/2} \int_0^\infty JS(J) \exp\left[-K(u, J)\right] dJ, \tag{15}$$

where we have introduced the variable $u = r^2$ and the functions

$$S(J) = c(J)P(J)\exp\left[E_{\min}(J)/c^2(J)\right] \tag{16}$$

and

$$K(u,J) = \frac{J^2/2u + \Phi(\sqrt{u})}{c^2(J)} = \frac{\Phi_{eff}(\sqrt{u},J)}{c^2(J)}, \tag{17}$$

with Φ_{eff} the effective potential.

In Appendix B we show that by multiplying Eq. (15) by $\exp[K(u,J')]$ and by integrating along the imaginary axis in the complex variable $z = \partial K(u,J')/\partial J'$ (for real J') we obtain the expression:

$$(2\pi)^{3/2} J' S(J') \approx \frac{1}{2\pi i}\int_{\mathbf{C}} u\rho(\sqrt{u})\frac{\partial z}{\partial u}\exp\left[K(u,J')\right]du, \tag{18}$$

which, for small values of ϵ, gives the desired inversion, i.e. an expression for the normalization factor $P(J)$ leading to the specified density distribution $\rho(r)$. Here the contour **C** corresponds to the path of integration in the variable u, which is reduced to a small circle in the complex plane in the vicinity of $u = 0$ (residue). Such an integral can be performed numerically.

In the following we focus on a specific demonstration for the case where the basic density corresponds to an isochrone model, but the method appears to be fairly general with respect to the choice of the density distribution (see Appendix B). Here we may recall that in the different context of finding exact inversion procedures, but within the general goal of constructing self-consistent stellar dynamical models, the use of contour integrals has found a recent interesting application by Hunter & Qian (1993).

The first method (fixed functional form of distribution function) leads to a normalization function P that does not guarantee uniform support to a given ρ at all radii, while the second method (contour integration) does. From a technical point of view, the reason why this occurs is explained in detail in the last paragraph of Appendix A and the first paragraph of Appendix B.

3. Application to isochrone potentials

We now investigate in detail the application to the isochrone potential. The isochrone models (Hénon 1959) are convenient in that they have a realistic outer density profile, while involving simple analytical expressions. Therefore they have often been used in studies of stellar dynamics, mainly for systems with radially biased velocity dispersion (e.g., Gerhard 1991; Saha 1991).

3.1. Basic analytical relations

The isochrone potential is defined as:

$$\Phi(r) = -\frac{GM}{b + \sqrt{b^2 + r^2}}. \tag{19}$$

In the following we shall provide formulae where the units for Φ and length are GM/b and b respectively. Thus the quantities $r_0(J)$ and $E_{\min}(J)$ entering the distribution function (1) become:

$$E_{\min}(J) = -\frac{1}{2(J/2 + \sqrt{1 + J^2/4}\,)^2}, \tag{20}$$

$$r_0(J) = \left[2J^2(1 + J^2/4) + J(J^2+2)\sqrt{1 + J^2/4}\,\right]^{1/2}, \tag{21}$$

and the quantities ρ and κ that appear in the definition (9) of $P(r_0)$ are:

$$\rho(r_0) = \frac{1 + 2\sqrt{1 + r_0^2}}{\left(\sqrt{1 + r_0^2}\right)^3\left(1 + \sqrt{1 + r_0^2}\right)^2}, \tag{22}$$

$$\kappa(r_0) = (1 + r_0^2)^{-3/4}. \tag{23}$$

Note that in these units the value of the total mass is $M = 4\pi$ and the half-mass radius is given by $r_M \approx 3.06$.

Finally, in the following models we keep the scale-length for the onset of tangentially biased pressure fixed by taking $J_1 = 1$ in the definition (8) of the quantity $\hat{c}$. Thus ϵ is the only parameter that will be changed in our model survey, varying from 0.05 up to 0.30.

3.2. Models with fixed functional form of the distribution function

We now consider the first option described in the last paragraph of Sect. 2.2, and we do so by keeping all quantities appearing in the definition (9) of $P(r_0)$ fixed by the expressions given in the previous subsection. Thus the only updated quantity in the form of the distribution function subject to the iteration procedure described in Sect. 2.3 is the potential Φ entering E and $E_{\min}(J)$ in the exponent of Eq. (1).

The computation of the integral over tangential velocities has been performed using cubic splines on a logarithmic mesh, with the smallest step–size at $v_\perp = v_{\perp 0} = r\Omega(r)$, as also suggested by the saddle point analysis of Appendix A.

Convergence is reached typically after 5 to 10 iterations, with the virial theorem verified at the 0.01 percent accuracy level.

In the central region, the resulting density exhibits a significant deviation from the isochrone profile (Fig. 1). As expected, the overall deviation is larger for larger values of ϵ. On the other hand, the $\epsilon \to 0$ limit is not trivial (see the last paragraph of Appendix A); this is illustrated by the fact that the deviations from the isochrone density occur on a smaller and smaller radial scale but, for the smallest values of ϵ ($\epsilon < 0.1$), the density profile develops a significant non-monotonicity. All models present a small "bump" ($< 2\%$) at very small radii ($r \simeq 0.002\ r_M$).

The profiles of the anisotropy parameter α defined by Eq. (5) are shown in Fig. 2. Close to the center (Fig. 2b), in the region where the deviations in the density distribution occur, these profiles differ from the asymptotic estimates given by Eq. (6). In addition, the cases with the largest values of ϵ may even show a

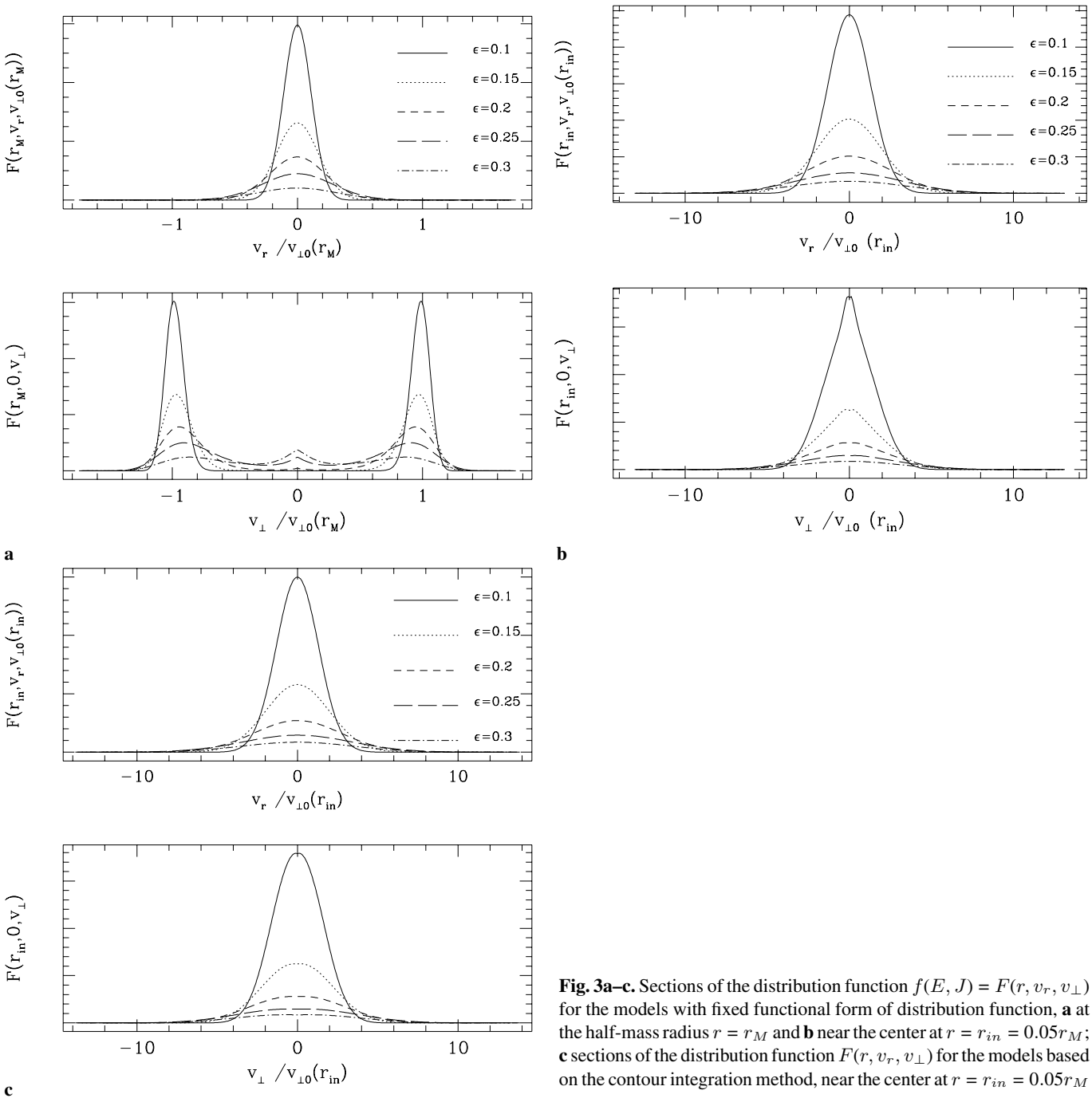

Fig. 3a–c. Sections of the distribution function $f(E, J) = F(r, v_r, v_\perp)$ for the models with fixed functional form of distribution function, **a** at the half-mass radius $r = r_M$ and **b** near the center at $r = r_{in} = 0.05 r_M$; **c** sections of the distribution function $F(r, v_r, v_\perp)$ for the models based on the contour integration method, near the center at $r = r_{in} = 0.05 r_M$

significant radial range where the velocity dispersion is radially biased.

In order to appreciate the structure of velocity space associated with our models better, in Fig. 3 we show some relevant sections of the distribution function at two different radii. While the central cuts indicate that the models are reasonably isotropic (Fig. 3b), a two-horned structure in the tangential velocity plane is clearly seen at $r = r_M$ (Fig. 3a). Again, for the cases with the largest values of ϵ an additional feature at $v_\perp = 0$ develops which may be traced to the population of radial orbits originating from the center.

In Fig. 4 the anisotropy structure of our sequence of models is illustrated in a different form that gives a simple way of appreciating the size of the anisotropy involved with cases of direct astrophysical interest (in particular, compare the case of $\epsilon = 0.2$ with Fig. 4 of the paper by Bertin et al. 1994a).

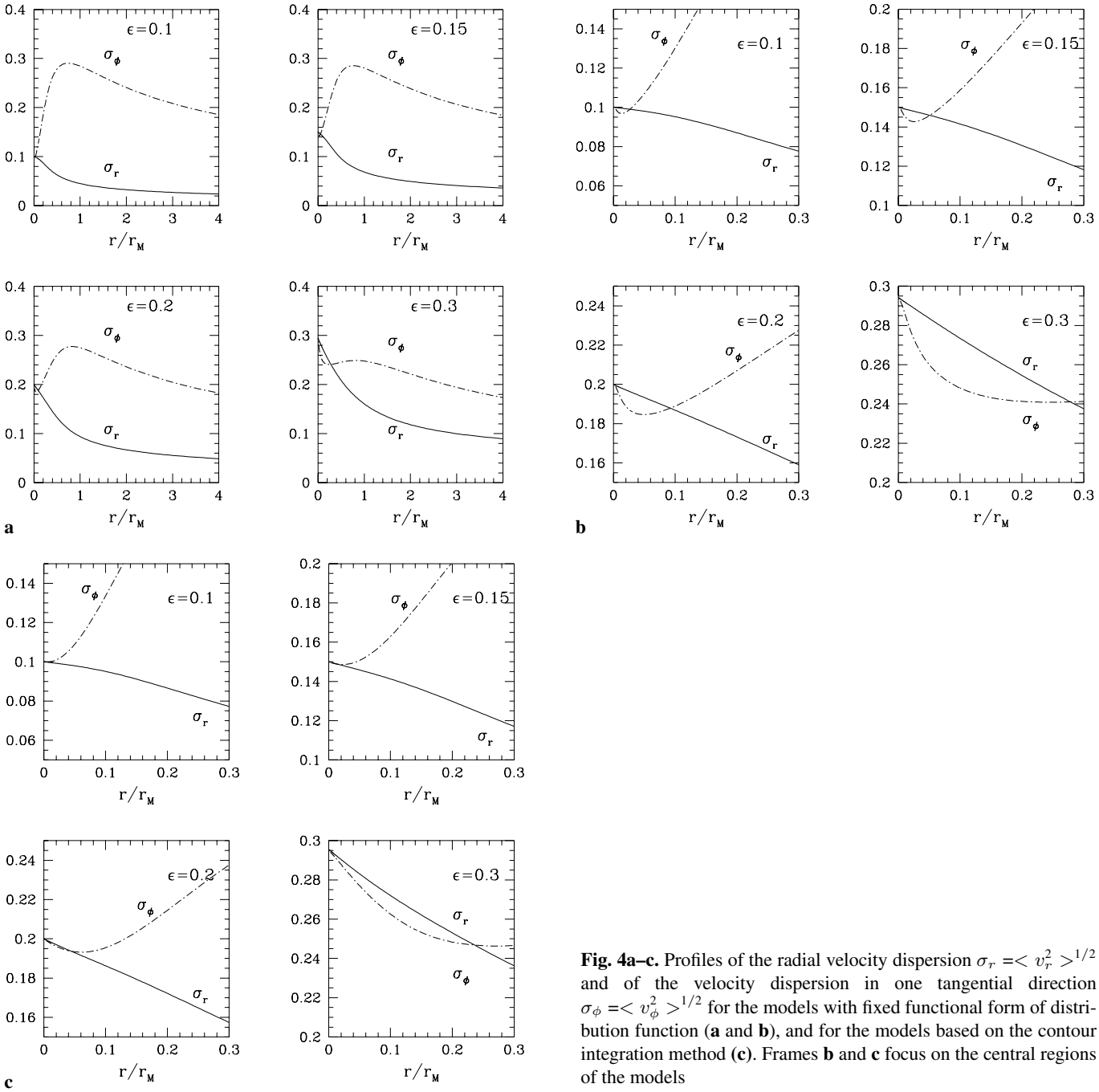

Fig. 4a–c. Profiles of the radial velocity dispersion $\sigma_r = < v_r^2 >^{1/2}$ and of the velocity dispersion in one tangential direction $\sigma_\phi = < v_\phi^2 >^{1/2}$ for the models with fixed functional form of distribution function (**a** and **b**), and for the models based on the contour integration method **(c)**. Frames **b** and **c** focus on the central regions of the models

3.3. Models based on the contour integration method

Proceeding with the second option described in the last paragraph of Sect. 2.2, we consider the models constructed following the method outlined in Sect. 2.4. The isochrone density profile is then reproduced rather accurately down to the center. Judging from the closeness between the density computed by the inversion and the isochrone density, this method appears to work reasonably well even for relatively large values of $\epsilon \approx 0.3$.

In Figs. 2(c), 3(c), and 4(c) we show the various profiles for comparison with the models obtained with the other method.

Numerical properties of the two classes of models described in this and in the previous subsection are summarized in Table 1. Table 2 lists the kinematic properties, and, in particular, the values of the global anisotropy parameter $2K_r/K_t$ (cf. Bertin et al. 1994b), where K_r and K_t are the total kinetic energies relative to radial and tangential motions respectively, and of the scale-length r_α defined as the location where $\alpha(r) = -1$.

4. Conclusions

In this paper we have provided a general and flexible procedure to construct self-consistent spherical equilibrium models

Table 1. Numerical parameters of the models compared to those of the initial isochrone potential, based on a construction that keeps the central density fixed: models based on Eq. (9) for $P(r_0)$ (left) and models based on the contour integration method (right). The value of the virial ratio is indicated only when different from unity by more than 10^{-4}

ϵ	M/M_{iso}	r_M/r_{M-iso}	$Virial$	M/M_{iso}	r_M/r_{M-iso}	$Virial$
0.05	1.004	1.0007		1.0005	0.9994	
0.1	1.014	1.003		1.002	0.994	
0.15	1.032	1.004		1.006	0.985	
0.2	1.061	1.005		1.013	0.971	
0.25	1.11	1.025	1.00015	1.036	0.970	
0.3	1.24	1.133	1.0008	1.187	1.142	1.0003

Table 2. Kinematical parameters of the models: models based on Eq. (9) for $P(r_0)$ (left) and models based on the contour integration method (right)

ϵ	r_α/r_M	$\alpha(r_M)$	$\alpha(2r_M)$	$2K_r/K_t$	r_α/r_M	$\alpha(r_M)$	$\alpha(2r_M)$	$2K_r/K_t$
0.05	0.03	−322	−439	0.011	0.03	−322	−439	0.011
0.1	0.08	−77	−106	0.045	0.07	−78	−108	0.045
0.15	0.13	−31	−45	0.105	0.12	−31	−44	0.107
0.2	0.21	−15	−23	0.197	0.19	−14	−21	0.204
0.25	0.33	−7.2	−12	0.330	0.31	−6.7	−10	0.351
0.3	0.49	−3.2	−5.5	0.529	0.45	−3.0	−4.2	0.583

of stellar systems populated by stars in quasi-circular orbits. The method is relatively simple and intuitive, because it makes use of and brings out clearly all the well known properties of systems where the epicyclic approximation is applicable. Starting from a given density profile, two different options have been pursued, one where priority is given to retain a simple functional form for the distribution function in phase space, and another where the models that are constructed have a density distribution that is very close to the initial chosen profile. The method has been demonstrated in quantitative detail by constructing sequences of equilibrium models with varying degrees of tangential bias in the pressure tensor distribution, all based on the isochrone potential. This study is meant to be the starting point for future stability analyses and may be also of some interest in the discussion of some spectroscopic data now available for many elliptical galaxies.

Acknowledgements. We would like to thank S. Caracciolo for helpful discussions and J. Schmidt for suggesting the idea at the basis of the method outlined in Appendix B. This work has been partially supported by CNR and MURST of Italy.

Appendix A: the saddle-point evaluation of the density integral

The following saddle-point analysis justifies our choice of the normalization function $P(J)$ as given by Eqs. (4) and (9). We start from the definition of the density:

$$\rho(r) = \int f d^3v = \frac{2\pi}{r^2}\int_0^{\bar{J}} JdJ\ P(J)$$
$$\times \exp\left(-\frac{\frac{J^2}{2r^2}+\Phi(r)-E_{\min}(J)}{c^2(J)}\right)\mathscr{I}_0, \qquad \text{(A24)}$$

where the integral in the radial velocity $\mathscr{I}_0$ is:

$$\mathscr{I}_0 = 2\int_0^{\bar{v}_r} dv_r \exp\left(-\frac{v_r^2}{2c^2(J)}\right); \qquad \text{(A25)}$$

here $\bar{J} = r\sqrt{-2\Phi(r)}$ and $\bar{v}_r = \sqrt{-2\Phi(r)-J^2/r^2}$. Along the positive real J-axis, the phase of the exponential function in Eq. (A24) is stationary at J_0 defined by the relation $J_0 = r^2\Omega(r)$. Since, for $\epsilon \to 0$ the quantity $\bar{J}/rc(J_0)$ goes to infinity uniformly in r, we can effectively set the upper integration limits in Eqs.(A24) and (A25) to infinity. Thus Eq. (14) follows.

The argument of the exponential in Eq. (A24) vanishes at $J = J_0$ and can be expanded to give:

$$\rho(r) \sim \frac{(2\pi)^{3/2}}{r^2}\int_0^\infty JdJ\ P(J)c(J)$$
$$\times \exp\left[-\frac{\lambda^2(r)}{r^2c^2(J_0)}(J-J_0)^2+\ldots\right]. \qquad \text{(A26)}$$

Here the function λ^2 is defined as:

$$\lambda^2(r) = [1 - r^2E''_{\min}(J_0)]/2 = 2\Omega^2/\kappa^2. \qquad \text{(A27)}$$

Note that the function $\lambda^2(r)$ is well behaved. Let us now introduce the scaled velocity variable $\xi = (J-J_0)/(\epsilon r)$ and further expand the argument of the integral:

$$\rho(r) \sim (2\pi)^{3/2}\epsilon^2\int_{-a}^{\infty} d\xi\ [v_{\perp 0}\mathscr{P}(J_0) + \epsilon\xi(\mathscr{P}(J_0)$$
$$+J_0\mathscr{P}'(J_0)+\ldots)] \times \exp\left[-\frac{\lambda^2(r)}{\hat{c}^2(J_0)}\xi^2+\ldots\right] \qquad \text{(A28)}$$

with $\mathscr{P} = P(J)\hat{c}(J)$, $v_{\perp 0} = J_0/r = r\Omega(r)$, and $a = v_{\perp 0}/\epsilon$, and we recall that $c = \epsilon\ \hat{c}$. This leads to the final expression:

$$\rho(r) \sim (2\pi)^{3/2}\epsilon^2\mathscr{P}(J_0)\left[v_{\perp 0}\mathscr{I}_1 + \epsilon\ \frac{d\ln(J\mathscr{P})}{d\ln J}\bigg|_{J_0}\mathscr{I}_2\right], \quad \text{(A29)}$$

where:

$$\mathscr{I}_1 = \frac{(\pi)^{1/2}\hat{c}(J_0)}{2\lambda}[1 - \mathrm{erf}(-a\lambda/\hat{c})] \quad \text{(A30)}$$

and

$$\mathscr{I}_2 = \frac{\hat{c}^2(J_0)}{2\lambda^2}\exp[-(a\lambda/\hat{c})^2]. \quad \text{(A31)}$$

The two limits, $r \to 0$ and $r/\epsilon \to \infty$ yield the well known normalization of an isotropic Maxwellian and the epicyclic normalization of Eq. (4), respectively. These limits justify our choice (10) for the function $g(r_0)$. The limitation of this saddle-point method is recognized in the fact that the assumption of slow variations of the quantity $\mathscr{P}$ is violated in the region where $r = O(\epsilon)$, because the two integrals $\mathscr{I}_1$ and $\mathscr{I}_2$ are found to present large derivatives there. One possible way out that has been attempted has been to introduce an appropriate "fudge factor" to compensate for the undesired fast variations; in practice, the problem is best resolved by a contour integration, as illustrated in the following Appendix B.

Appendix B: contour integration

If we want to generate models that reproduce the chosen density distribution more accurately at small radii, we can proceed by an approximate inversion of the relationship between the density and the distribution function in the following way (as suggested to us by J. Schmidt). The method is still based on the smallness of the parameter ϵ, but, by means of a suitable transformation of the relevant integrals, the approximations are all carried out in one integral that does not depend on the unknown normalization factor P.

We start from Eq. (15)

$$u\rho(\sqrt{u}) = (2\pi)^{3/2}\int_0^\infty JS(J)\exp[-K(u,J)]dJ, \quad \text{(B32)}$$

where the quantities $u, K(u,J)$ and $S(J)$ are defined in Sect. 2.4. We multiply both sides by $\exp[K(u,J')]$ and integrate them with respect to the "radial" variable

$$z \equiv \frac{\partial K(u,J')}{\partial J'} \quad \text{(B33)}$$

along the imaginary axis $i\Re$ at constant J'. By exchanging the order of integration on the right hand side, this procedure leads to

$$\frac{1}{2\pi i}\int_{i\Re} u\rho(\sqrt{u})\exp[K(u,J')]dz = \quad \text{(B34)}$$

$$(2\pi)^{3/2}\int_0^\infty dJ\,JS(J)\frac{1}{2\pi i}\int_{i\Re}\exp[-K(u,J)+K(u,J')]dz.$$

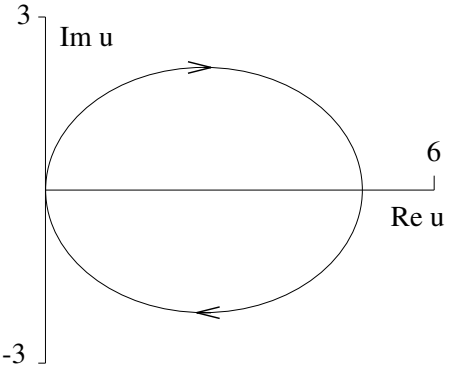

Fig. 5. Integration path in the complex u-plane, illustrated for the isochrone potential at $J' = 1$. This corresponds to the integration in the z-variable along the imaginary axis

The inversion formula

$$\frac{1}{2\pi i}\int_{i\Re} u\rho(\sqrt{u})\exp[K(u,J')]dz \approx (2\pi)^{3/2}\ J'S(J') \quad \text{(B35)}$$

follows by noting that, to leading order in ϵ,

$$\frac{1}{2\pi i}\int_{i\Re}\exp[-K(u,J)+K(u,J')]\ dz \approx \delta(J-J'). \quad \text{(B36)}$$

This result can be derived by expanding $[-K(u,J)+K(u,J')]$ for $J' \approx J$, provided the ratios $(1/z)\partial^n z/\partial J'^n$ between the following coefficients and the first in the Taylor expansion be bounded.

In order to evaluate the inverse integral transform (B35) explicitly, it is more convenient to bring the integral over z along the imaginary axis into an integral over $u = u(z)$. The detailed form of the integration path in the complex u-plane depends on the explicit form of the potential $\Phi(\sqrt{u})$, but its main features are quite general and are governed by the contribution arising from the centrifugal potential, which dominates at $z \to \pm i\infty$, i.e., $u \mp i0$, and by the crossing of the real u-axis at $u = u_R$ for $z = 0$.

The resulting ovaloid shape of the integration path in the complex u-plane is shown for the case of the isochrone potential in Fig. 5. The integrand in Eq. (B35) has neither poles nor branch-points inside this ovaloid, but has an essential singularity at $u = 0$. In the half-plane to the left (negative real-part of u) of the essential singularity, the integrand in Eq. (B35) is exponentially small. Then, the integration path can be deformed so as to fully encircle the singularity at $u = 0$ and the inversion formula (B35) becomes

$$(2\pi)^{3/2}\ J'S(J') \approx \mathscr{R}es\left[u\rho(\sqrt{u})\exp(K(u,J'))\frac{\partial^2 K(u,J')}{\partial J'\partial u}\right]_{u=0}, \quad \text{(B37)}$$

where the residue $\mathscr{R}es$ at $u = 0$ is best computed numerically by integrating Eq. (B35) along a path enclosing $u = 0$ and $u = u_L(J')$ on the positive real axis such that $K(u_L, J') \leq 0$. This completes the derivation of Eq. (18).

References

Bender R., Saglia R.P., Gerhard O., 1994, MNRAS 269, 785
Bertin G., Bertola F., Buson L.M., et al., 1994a, A&A 292, 381
Bertin G., Pegoraro F., Rubini F., Vesperini E., 1994b, ApJ 434, 94
Bertin G., Stiavelli M., 1993, Rep. Prog. Physics 56, 493
Cuddeford P., 1991, MNRAS, 253, 414
Dejonghe H., 1989, ApJ 343, 113
Fridman A.M., Polyachenko V.L., 1984, Physics of Gravitating Systems (2 Volumes), Springer-Verlag, Berlin
Gerhard O., 1991, MNRAS 250, 812
Hénon M., 1959, Ann. d'Astrophys. 22, 126
Hénon M., 1973, AA 24, 229
Hunter C., Qian E., 1993, MNRAS 262, 401
Louis P.D., 1993, MNRAS 261, 283
Merritt D., 1985a, AJ 90, 1027
Merritt D., 1985b, MNRAS 214, 25p
Osipkov L.P., 1979, Pis'ma Astr. Zh. 5, 77
Palmer P.L., 1994, Stability of Collisionless Stellar Systems, Kluwer, Dordrecht
Saha P., 1991, MNRAS 248, 464
Shu F.H., 1969, ApJ 158, 505
Tonry J.L., 1983, ApJ 266, 58